Neurotherapeutics (2021) 18:2664–2681
https://doi.org/10.1007/s13311-021-01140-4

ORIGINAL ARTICLE

Crosstalk Among NLRP3 Inflammasome, ET_BR Signaling, and miRNAs in Stress-Induced Depression-Like Behavior: a Modulatory Role for SGLT2 Inhibitors

Radwa N. Muhammad[1] · Lamiaa A. Ahmed[1] · Rania M. Abdul Salam[1,2] · Kawkab A. Ahmed[3] · Amina S. Attia[1]

Accepted: 5 October 2021 / Published online: 18 October 2021

Abstract

Depression is an overwhelming health concern, and many patients fail to optimally respond to available standard therapies. Neuroplasticity and blood–brain barrier (BBB) integrity are the cornerstones of a well-functioning central nervous system, but they are vulnerable to an overly active NLRP3 inflammasome pathway that can also indirectly trigger the release of ET-1 and contribute to the ET system disturbance, which further damages stress resilience mechanisms. Here, the promising yet unexplored antidepressant potential of dapagliflozin (Dapa), a sodium–glucose co-transporter-2 inhibitor, was investigated by assessing its role in the modulation of the NLRP3 inflammasome pathway and ET_BR signal transduction, and their impact on neuroplasticity and BBB integrity in an animal model of depression. Dapa (1 mg/kg/day; p.o.) with and without BQ-788 (1 mg/kg/day; i.p.), a specific ET_BR blocker, were administered to adolescent male Wistar rats exposed to a 5-week chronic unpredictable stress protocol. The depressive animals demonstrated marked activation of the NLRP3 inflammasome pathway (NF-κB/NLRP3/caspase-1/IL/TNF-α), which was associated with both peripheral and central inflammatory responses. The ET system was disrupted, with noticeable reduction in miR-125a-5p and ET_BR gene expression. Cortical ZO-1 expression was downregulated under the influence of NLRP3/TNF-α/miR-501-3p signaling, along with a prominent reduction in hippocampal BDNF and synapsin-1. With ET_BR up-regulation being a cornerstone outcome, Dapa administration efficiently created an overall state of resilience, improved histopathological and behavioral variables, and preserved BBB function. These observations were further verified by the results obtained with BQ-788 co-administration. Thus, Dapa may exert its antidepressant action by reinforcing BBB integrity and promoting neuroplasticity through manipulation of the NLRP3/ET-1/ET_BR/BDNF/ZO-1 axis, with a significant role for ET_BR signaling.

Keywords Depression · Dapagliflozin · SGLT2 · NLRP3 · ET_BR · Neuro-inflammation · miR-501-3p · miR-125a-5p

Introduction

Major depressive disorder (MDD) is currently one of the leading causes of disability and suicidal death worldwide [1, 2], and despite extensive research and massive improvements in mental health, the nature of MDD remains ambiguous. Moreover, about two-thirds of MDD patients fail to optimally respond to currently available standard therapies, and many of them suffer from treatment-resistant depression [2, 3]. MDD is a multi-factorial disorder which involves not only emotional disturbance, but also cognitive and functional impairments as integral features of this heterogeneous disorder [4]. Therefore, it greatly sabotages the quality of life and negatively affects the productivity of patients [5]. Depression can be further complicated by presence of other comorbidities—one of a major concern is diabetes [2, 6]. Studies have demonstrated the bi-directional relationship between the two disorders, which is partially owed to some shared pathological mechanisms that are involved in their progression [6].

Most importantly, the integrity of the blood–brain barrier (BBB) is crucial for the well-being of the central nervous

✉ Radwa N. Muhammad
radwa.nasser@pharma.cu.edu.eg

[1] Department of Pharmacology and Toxicology, Faculty of Pharmacy, Cairo University, Cairo 11562, Egypt

[2] Department of Biology, School of Pharmacy, New Giza University, Giza, Egypt

[3] Pathology Department, Faculty of Veterinary Medicine, Cairo University, Giza 12211, Egypt

system (CNS). However, both local and systemic inflammations represent major threats to the BBB and contribute to its breakdown, with subsequent infiltration of immune cells, accumulation of waste, and disruption of neuronal function [7, 8]. Specifically, activation of the nucleotide-binding oligomerization domain, leucine-rich repeat, and pyrin domain-containing protein (NLRP)-3 inflammasome is linked to BBB disruption, neuro-inflammation, and impaired neurogenesis [9]. The NLRP3 inflammasome is a multimeric protein complex and a cytosolic sensor that activates inflammatory pro-caspase-1. It responds to a wide array of endogenous and exogenous danger signals, including stress, and its dysregulation is implicated in a heterogeneous group of disorders [10, 11]; thus, it is considered a promising therapeutic target in depression [12].

Interestingly, only a few previous studies have addressed the link between activation of the NLRP3 inflammasome pathway and disturbances in the endothelin (ET) system [13–15]. Specifically, disruption of the ET system in the brain is linked to multiple CNS pathologies [16]. ET-1 in the brain, via its major receptors ET_AR and ET_BR, mediates a complex mixture of both detrimental and beneficial effects that range from brain ischemia and disruption of the BBB to neuronal survival [15] and neurogenesis [16]. It has been demonstrated that ET_BR signaling is associated with neuronal survival and neurotrophins production, even though it can also increase BBB permeability [16–18]. Nevertheless, increasing evidence points to positive outcomes of ET_BR stimulation rather than its blockade [16, 17, 19, 20].

Notably, ET-1 synthesis is controlled by various factors, including inflammatory mediators such as tumor necrosis factor (TNF)-α, interleukin (IL)-1β, and microRNAs (miRNAs), especially miR-125a, which was found to be negatively associated with ET-1 gene expression [21]. Interestingly, miR-125a-5p is also positively correlated with the formation of tight junction (TJ) complexes between zonula occludens (ZO)-1 and vascular endothelial cadherin, thus maintaining BBB integrity [22]. Another miRNA, namely, miR-501-3p, is an important intermediate in this process, and it has been found to directly inhibit ZO-1 after being upregulated by TNF-α [23, 24].

Thus, current attempts to develop drugs that specifically target treatment-resistant depression should focus on these pathological pathways rather than merely addressing deficiencies in monoamine neurotransmitters [2]. Furthermore, hippocampal neurogenesis is recognized in depression and is no longer limited to neurodegenerative disorders; congruently, the neurotrophic hypothesis of depression describes a relationship between low levels of neurotrophic factors and vulnerability to stress [8, 25].

Dapagliflozin (Dapa) is an inhibitor of the sodium–glucose co-transporter-2 (SGLT2) and a novel class of oral antidiabetic drug that represents a breakthrough in the management of type 2 diabetes mellitus [26–28]. Since their release, continuous research has revealed promising health outcomes of SGLT2 inhibitors in multiple organs, including cardiovascular and renal systems [28]. However, recent attention has been directed toward their beneficial effects on the brain [29–31], as SGLT2 expression has been demonstrated in multiple brain regions, including the hippocampus and endothelial cells in the BBB [30]. Studies have also demonstrated the neuroprotective potential of SGLT2 inhibitors, highlighting their antioxidant, anti-inflammatory, and antiapoptotic effects, in addition to improving angiogenesis and neurogenesis regardless of their glycemic control benefits [29–33]. However, the mechanisms underlying the effects of SGLT2 inhibitors on depression are still elusive.

Based on the evidence provided, the main aim of this study was to evaluate the effects of Dapa as a therapeutic modality in an animal model of depression. Specifically, we explored its role on the activation of the NLRP3 inflammasome, ET_BR signaling, and impact of these on neurotrophins production and BBB integrity. As the relationship between SGLT2 inhibitors and the ET system is not yet clear, our secondary aim was to investigate whether BQ-788, a specific ET_BR blocker, would at least in part negatively affect the antidepressant outcomes provoked by Dapa administration.

Materials and Methods

Animals

Fifty-six male Wistar rats in their early adolescence (30–33 days old) [34, 35], and weighing between 105 and 120 g, were used in this study. Rats were obtained from the animal facility of the National Research Center (Giza, Egypt), and were trained using the open field test (OFT) and the sucrose preference test (SPT) to exclude animals showing extreme or abnormal behavior.

A one-week acclimation period preceded the experimental protocol, during which animals were provided free access to standard chow and water ad libitum and housed under controlled environmental conditions with a room temperature of 25° ± 2 °C, relative humidity of 60% ± 10%, and a 12-h light–dark cycle [36]. All the study procedures strictly complied with the Guide for the Care and Use of Laboratory Animals published by the US National Institute of Health (NIH Publication No. 85–23, revised 2011) and were approved by the Ethics Committee for Animal Experimentation at the Faculty of Pharmacy, Cairo University (Permit Number: PT 2574). All efforts were made to minimize suffering of the animals.

Drugs

Escitalopram (Escita) (reference antidepressant drug), Dapa, and BQ-788 were obtained from H. Lundbeck A/S (Copenhagen, Denmark), AstraZeneca pharmaceutical company (Cambridge, UK), and MedChemExpress (NJ, USA), respectively.

All drugs were daily prepared as fresh suspensions in normal physiological saline; Escita, 4 mg/ ml; Dapa, 0.5 mg/ ml; and BQ-788, 0.5 mg/ ml.

Chronic Unpredictable Stress Protocol

The chronic unpredictable stress (CUS) procedure was implemented to induce depression-like behavior in rats as a simulation of daily-life stressors in humans. As CUS protocols are highly variable among different studies, we chose the one with the least harm to animals, i.e., avoiding electric shocks, tail pinching, exposure to extreme temperatures, or applying unnecessarily long protocols. The implemented CUS regimen was a minor modification of that described by Sequeira-Cordero et al. [34]. Briefly, animals were exposed to a five-week stress protocol, starting from postnatal day 33, which consisted of the following seven stressors: food deprivation, water deprivation, sleep deprivation, cage tilting with minimal food and water access, wet bedding, physical restraint, and reversal of the light–dark cycle. Each stressor was applied only once every week, and to reduce predictability and adaptation, stressors were semi-randomly applied, and each lasted for 22 h.

Experimental Protocol

Rats were randomly allocated into five groups. All drug treatments were initiated from the second week of the CUS protocol and lasted for four consecutive weeks. Animals in the first group ($n = 10$) received normal physiological saline (1 ml/day; p.o) and served as the negative control (normal) group. Rats in groups 2–5 were exposed to CUS as previously described. Specifically, those in group 2 ($n = 13$) were left untreated except for daily saline administration to serve as the positive control group; animals in groups 3 and 4 ($n = 10$ each) were treated with Escita (10 mg/kg/day; p.o) [37] and Dapa (1 mg/kg/day; p.o) [29], respectively, while those in group 5 ($n = 13$) were co-treated with BQ-788 (1 mg/kg/day; i.p.) [38, 39] along with Dapa (BQ-788 was injected one hour before Dapa administration) (Fig. 1). Animals were constantly monitored for food and water intake and were weighed two times per week for assessing body weight changes. Additionally, blood glucose levels were assessed in the Dapa groups (4 and 5) bi-weekly and compared to that of the negative controls.

Behavioral Tests

By the end of the third week, rats were trained for both the SPT and the forced swimming test (FST). Appropriate days for training were chosen to avoid interference with the CUS protocol (Fig. 1). All tests were carried out between 8:00 a.m. and 12:00 noon, starting with the test that had the least stressful impact on the rats.

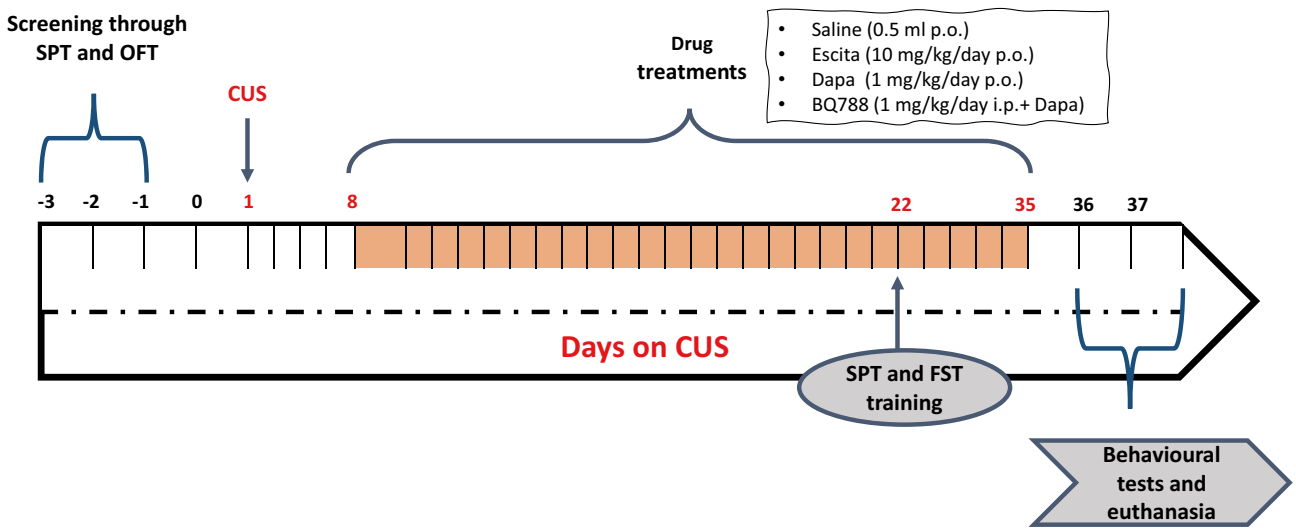

Fig. 1 Schematic illustration of experimental timeline. B BQ-788, CUS chronic unpredictable stress, Dapa dapagliflozin, Escita escitalopram, FST forced swimming test, OFT open field test, SPT sucrose preference test

Open Field Test

The OFT was originally developed to assess an animal's emotions [40]; however, its use is becoming popular in multiple areas of neuroscience. The test was carried out as described previously [36, 40, 41]. Briefly, the test was performed in a sound-attenuated room under dim white light with an overhead camera to monitor animal behavior. Each rat was gently placed in the central area of the open field and was allowed to freely explore the area for 5 min, during which locomotor activity was assessed based on the number of crossed squares, in addition to rearing behavior [40]. The box was cleaned between tests to eliminate possible bias caused by olfactory influences.

Sucrose Preference Test

The SPT is widely used to evaluate anhedonia, a core symptom in MDD [42], and the procedure described by *Casarotto and Andreatini* was followed [43]. Before initiating the procedure, rats were provided two identical bottles of 2% sucrose solution [44] as the sole source of drinkable fluid for two days to allow acclimatization to sucrose. This was followed by free access to standard food and water for two additional days. Next, animals were water-deprived for 16 h on the day before testing day, and on the testing day, each rat was individually housed for 1 h [41, 43, 45], and two identical bottles containing 100 ml of either 2% sucrose solution or tap water were provided. The position of the bottles was changed after 30 min during the test to avoid side preference. Sucrose preference for each rat was calculated according to the following formula:

$$\text{Sucrose preference} = (\text{Sucrose intake}/\text{Total fluid intake}) \times 100$$

The test was performed at baseline, in the mid-experimental period (3 weeks) to monitor CUS progression, and at the end of the experimental protocol. Rats showing sucrose preference of $< 65\%$ were categorized as anhedonic [42].

Forced Swimming Test

This behavioral test is widely used to assess the "despair" component of depression [40]. In the FST, rodents are exposed to an inescapable swimming situation where they are forced to swim in a water-filled cylindrical container till they eventually stop struggling after a period of active movement. The test was conducted as formerly described in different studies [36, 40]. Briefly, rats were trained to swim for 15 min, and on the next day, the test was performed under the same conditions, but testing time was limited to 5 min. Water was changed after each animal was tested and the cylinder was thoroughly rinsed. All animals were then dried and kept warm using a heating lamp to avoid hypothermia. The test was recorded, and total immobility time for each animal was calculated. Immobility time was defined as the duration for which the animal appears to be floating, stops moving, and only makes minor movements to keep its head above the water surface [46].

Preparation of Samples

After behavioral testing, rats were anesthetized using ketamine/xylazine (60/7.5 mg/kg; i.p.), blood samples were collected from the femoral vein for subsequent separation of sera using non-heparinized capillary tubes, and animals were euthanized by cervical dislocation under anesthesia. Hippocampi and cortices were isolated, washed, and dried for further processing, biochemical analyses, and histological evaluation.

Biochemical Analyses

Enzyme-Linked Immunosorbent Assays

Hippocampi/cortices ($n = 7-8$) were homogenized in ice-cold phosphate-buffered saline as 10% homogenates, and corresponding commercial kits were utilized, according to the manufacturers' protocols, to assess either serum levels or relevant tissue contents of the following biomarkers: serotonin (5-HT) (Cat# MBS9362408, MyBioSource, CA, USA), norepinephrine (NE) (Cat# MBS269993, MyBioSource, CA, USA), and dopamine (DA) (Cat# CSB-E08660r, Cusabio, Wuhan, China). Cusabio (Wuhan, China) ELISA kits were used for the assessment of IL-1β (Cat# CSB-E08055r) and IL-18 (Cat# CSB-E04610r). Additionally, the phosphorylated forms of the nuclear factor kappa (*p*-Ser536 NF-κB p65) and TNF-α were measured using Abcam (Cat# ab176647, Cambridge, UK) and Biospes (Cat# BEK1214, Chongqing, China) kits, respectively. Finally, kits obtained from MyBioSource (CA, USA) were used for ET-1 (Cat# MBS006526) and synapsin-1 (Cat# MBS761293) quantification, whereas BDNF was assessed using Elabscience kit (Cat# E-EL-R1235, Wuhan, China).

Colorimetric Assay for Caspase-1

Caspase-1 activity was evaluated colorimetrically using Novus Biologicals assay kit (Cat# NBP2-54815, CO, USA). Absorbance was measured at 405 nm, and results were expressed as pmol pNA/min/mg protein.

Quantitative Reverse Transcription Polymerase Chain Reaction

Hippocampi/cortices ($n = 6$) were homogenized in lysis buffer to assess gene expression of hippocampal NLRP3, ET_AR, ET_BR, miR-125a-5p, and cortical miR-501-3p. First,

for NLRP3, ET_AR, and ET_BR, total RNA was extracted from the respective tissues using the RNeasy Mini kit (Qiagen, Hilden, Germany), and its purity was tested spectrophotometrically using the NanoDrop® (ThermoFisher Scientific, MA, USA) at OD 260/280 nm. This was followed by reverse transcription of RNA into complementary DNA using the Titan One-Tube RT-PCR System (Cat# 11855476001, Sigma–Aldrich, MO, USA) as per manufacturer's instructions and qRT-PCR using Invitrogen SuperScript III Platinum qRT-PCR Kit™ (Cat# 11732088, Invitrogen, CA, USA). A similar process was followed for miRNA extraction using the mirVana™ PARIS™ kit (Cat# AM1556, Invitrogen, CA, USA); complementary DNA was retrieved using the TaqMan™ MicroRNA Reverse Transcription Kit (Cat# 4366596, Applied Biosystems, CA, USA), and qRT-PCR was carried out using the TaqMan™ MicroRNA Assay (Applied Biosystems, CA, USA) with Cat# 4427975 for miR-125a-5p and #4440886 for miR-501-3p. Primer sequences, accession numbers, and assay IDs are listed in Table 1. After qRT-PCR, relative expression of target genes was calculated using the $2^{-\Delta\Delta CT}$ formula, with β-actin as the housekeeping gene, except for miRNAs, where U6 was used.

Hippocampal and Cortical Histopathological Examination

Whole brain tissues of euthanized rats (3/group) were isolated, immediately immersed in 10% buffered formalin, dehydrated in graded alcohol, and embedded in paraffin.

Histopathological Scoring

Five-micrometer-thick sections of the hippocampi and cortices were obtained from the paraffin blocks, stained with hematoxylin and eosin (H&E) (Sigma–Aldrich, MO, USA), and assessed (3 fields/ animal) under light microscope (Leica Microsystems, Wetzlar, Germany) at 400 × magnification by investigators blinded to the sample. Neuropathological damage in the cerebral cortex and the hippocampus was graded from 0 to 4 as follows: 0, no lesions; 1, less than 10% area affected; 2, 20–30% area affected; 3, 40–60% area affected; 4, > 60% area affected [47, 48].

Cortical ZO-1 Immunoreactivity

Sections (3-μm-thick) were obtained from prepared blocks, dewaxed in xylene, and rehydrated. Antigen retrieval was performed using the microwave method, and after cooling, endogenous peroxidase activity was blocked by incubation in 3% hydrogen peroxide solution for 10 min. Samples were blocked with 5% BSA for 10 min to prevent non-specific protein binding, followed by overnight incubation at 4 °C with primary rabbit polyclonal anti-ZO-1 antibody (1:100; Cat# E-AB-18170, Elabscience, Wuhan, China), washing with buffer, and incubation with secondary biotinylated goat anti-rabbit IgG (1:200; ThermoFisher Scientific, MA, USA) for 1 h at room temperature. Specimens were again buffer-washed and incubated with peroxidase-conjugated streptavidin for another hour. Immunoreactive ZO-1 bearing cells were visualized using the 3,3′-diaminobenzidine (DAB) Pierce™ Substrate Kit (ThermoFisher Scientific, MA, USA), and the prepared sections were then counterstained with hematoxylin, dried, and covered. Quantification of cortical ZO-1 and morphometric analysis were carried out by determining percentage area expression of ZO-1 in five random fields per animal using the Leica Qwin 500 Image Analyzer software (Leica Microsystems, Wetzlar, Germany).

Table 1 Primer sequences, access numbers, and assay IDs for qRT-PCR

mRNA genes			
ID	**Access#**	**Primer sequence**	**Size (bp)**
NLRP3	NM_001191642.1	F: 5′-TGCTCTTCACTGCTATCAAGC CCT-3′ R: 5′-ACAAGCCTTTGCTCCAGACCC TAT-3′	283
ET_AR (EDNRA)	NM_012550	F: 5′-GTCGAGAGGTGGCAAAGACC-3′ R: 5′-ACAGGGCGAAGATGACAACC-3′	64
ET_BR (EDNRB)	NM_017333	F: 5′-GATACGACAACTTCCGCTCCA-3′ R: 5′-GTCCACGATGAGGACAATGAG-3′	86
β-actin	NM_031144.3	F: 5′-CGTTGACATCCGTAAAGACCTC-3′ R: 5′-TAGGAGCCAGGGCAGTAATCT-3′	302
miRNA genes			
ID	**miRBase access#**	**Target RNA sequence**	**Assay ID**
rno-miR-125a-5p	MIMAT0000829	UCCCUGAGACCCUUUAACCUGUGA	002,198
rno-miR-501-3p	MIMAT0017198	AAUGCACCCGGGCAAGGAUUUGG	464079_mat
U6	Access# NCBI: NR_004394		

Statistical Analyses

All statistical analyses and graphical illustrations were performed using GraphPad Prism® software ver. 6 (GraphPad Software Inc., USA). For parametric data, comparisons of means were done using one-way analysis of variance (ANOVA), except for body weight gain, which was analyzed by two-way ANOVA, followed by the Tukey–Kramer multiple comparison test, where data were presented as means ± standard error of mean (SEM). For non-parametric data (OFT and histopathological scoring), Kruskal–Wallis followed by Dunn's multiple comparison tests were used instead, and data in this case were expressed as the median and range (min–max). The probability limit was set at $P < 0.05$ for all comparisons and was accepted as being statistically significant.

Results

In this set of experiments, one group of normal animals received Dapa (without CUS) and was examined concurrently with the other groups. However, no significant differences were observed in these animals compared to the negative control group in all parameters, and hence, comparisons were made relative to negative controls, and data for this group is not graphically represented.

Survival and Body Weight Gain

The CUS procedure was detrimental to both survival and weight gain as it resulted in ≈15% mortality and least weight gain (only ≈39% by week 5 from week 0). Both Dapa and Escita co-treatments significantly improved weight gain and resulted in no mortality. Notably, BQ-788 + Dapa produced results comparable to those with CUS alone (Table 2; Fig. 2a).

Table 2 Mortality % observed in the different treatment groups during the 5-week CUS protocol

Group	Mortality (%)
Control	0
CUS	15.4
CUS + Escita	0
CUS + Dapa	0
CUS + B + Dapa	15.4

B BQ-788, *CUS* chronic unpredictable stress, *Dapa* dapagliflozin, *Escita* escitalopram

Behavioral Alterations in Rats

No significant difference was observed in OFT among the groups in terms of locomotor activity, except for CUS + Dapa, which showed a significant increase in this variable compared to normal controls. Though all treatment groups showed increased locomotor activity, compared to normal controls, including CUS, this increase was not significant (Fig. 2b). Rearing frequency nearly followed a similar trend, with both Dapa and Escita groups showing significantly higher rearing behavior. Interestingly, BQ-788 + Dapa showed a significant reduction in rearing frequency when compared to CUS + Dapa.

In SPT, CUS-subjected rats showed a reduction in sucrose preference (41.81%), as compared to normal controls (85.64%), whereas CUS + Escita showed superior improvement in sucrose consumption than CUS + Dapa, and BQ-788 co-treatment with Dapa partially decreased the effect of the latter (Fig. 2c).

In FST, the CUS group displayed depression-like behavior, manifested as significant three-fold prolongation of immobility time as compared to the negative control group. While this was similarly normalized by the co-administration of either Dapa or Escita, leading to a considerable reduction in the immobility time by approximately 57% (compared to CUS), combined administration of BQ-788 + Dapa significantly abrogated the improvements due to Dapa and produced results similar to that seen with CUS (Fig. 2d).

Notably, results obtained from the OFT ruled out the possibility that changes induced by CUS alone or any of the treatments on the immobility time were due to non-specific effects on motor activity of the rats.

Monoamine Neurotransmitters in the Hippocampus

Stress exposure was associated with suppression of all monoamines in the hippocampus, especially 5-HT. Compared to negative controls, CUS-exposed rats showed 69% reduction in hippocampal 5-HT (Fig. 3a), 30% drop in DA (Fig. 3b), and 21.8% fall in NE (Fig. 3c). Results obtained with Dapa and Escita were nearly comparable, with no significant differences between the two groups. Notably, Dapa led to a 161.45% increase in hippocampal 5-HT and a 1.54-fold increase in DA content. Dapa co-treatment also augmented hippocampal NE by 53%. All these values were calculated as compared to CUS alone.

The ET_BR blocker, BQ-788, significantly attenuated the effects of Dapa on 5-HT and DA, but it did not affect its outcome on NE.

CUS-Induced Systemic Inflammation

CUS exposure led to a state of systemic inflammation (Fig. 4), reflected in the upsurge of serum levels of both IL-1β (211.27%) and IL-18 (215.25%), and co-treatment with Dapa attenuated these effects. Changes due to Dapa and Escita were similar, with no significant differences between the two treatments. Interestingly, BQ-788 did not significantly affect the anti-inflammatory potential of Dapa.

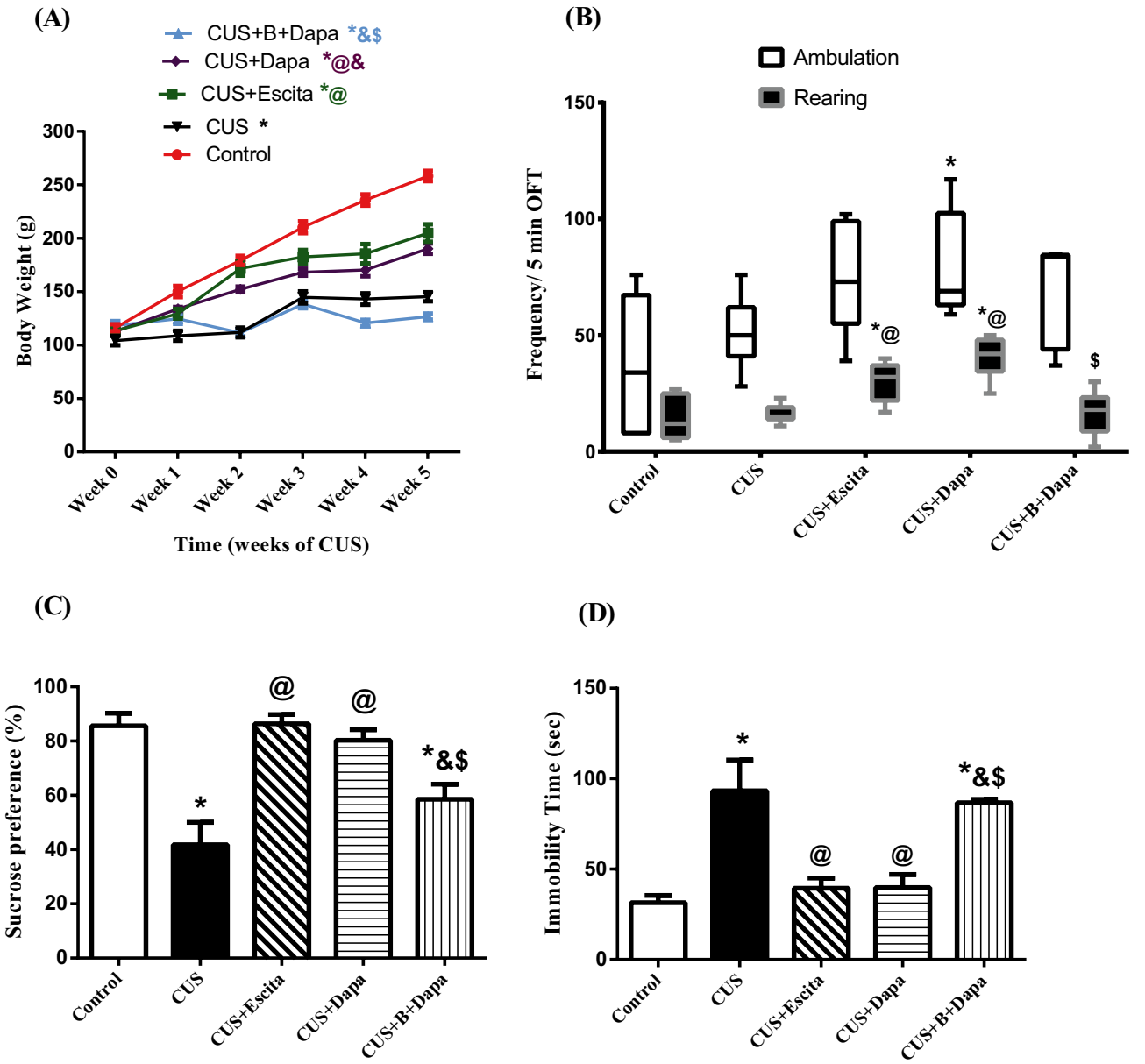

Fig. 2 Effect of the 5-week CUS protocol and co-treatments on **(a)** body weight gain, **(b)** ambulation and rearing frequencies in the OFT, **(c)** sucrose preference, and **(d)** immobility time during the FST. Parametric data is expressed as the mean of 10 − 11 experiments ± SEM, using one-way ANOVA with Tukey−Kramer multiple comparison post-test, except for body weight gain, where two-way ANOVA was used instead. Non-parametric data is presented as box and whiskers by median (min−max) and 25^{th}–75^{th} percentile values using Kruskal–Wallis test with Dunn's multiple comparison post-test; as compared to normal (*), CUS (@), Escita (&), and Dapa ($)-treated groups ($p < 0.05$). B BQ-788, CUS chronic unpredictable stress, Dapa dapagliflozin, Escita escitalopram, FST forced swimming test, OFT open field test

CUS-Associated NLRP3 Inflammasome Pathway Activation in the Hippocampus

Compared to normal controls, animals exposed to CUS showed a prominent increase in pyroptotic cell death components (Fig. 5), namely, *p*-NF-κB p65 (Ser536; 314.47%), with consequent increase in the mRNA expression of NLRP3 (630.05%), caspase-1 activity (5-fold), IL-1β (3.7-fold), and IL-18 (2.76-fold).

Comparatively, both Dapa and Escita showed outstanding suppression of this pathway, with Dapa displaying superior results; specifically, compared to CUS rats, Dapa suppressed *p*-NF-κB p65 (Ser536) by 78.78%, NLRP3 by 67.94%, caspase-1 activity to one-third, IL-1β by 64.34%, and IL-18 by 52.64%.

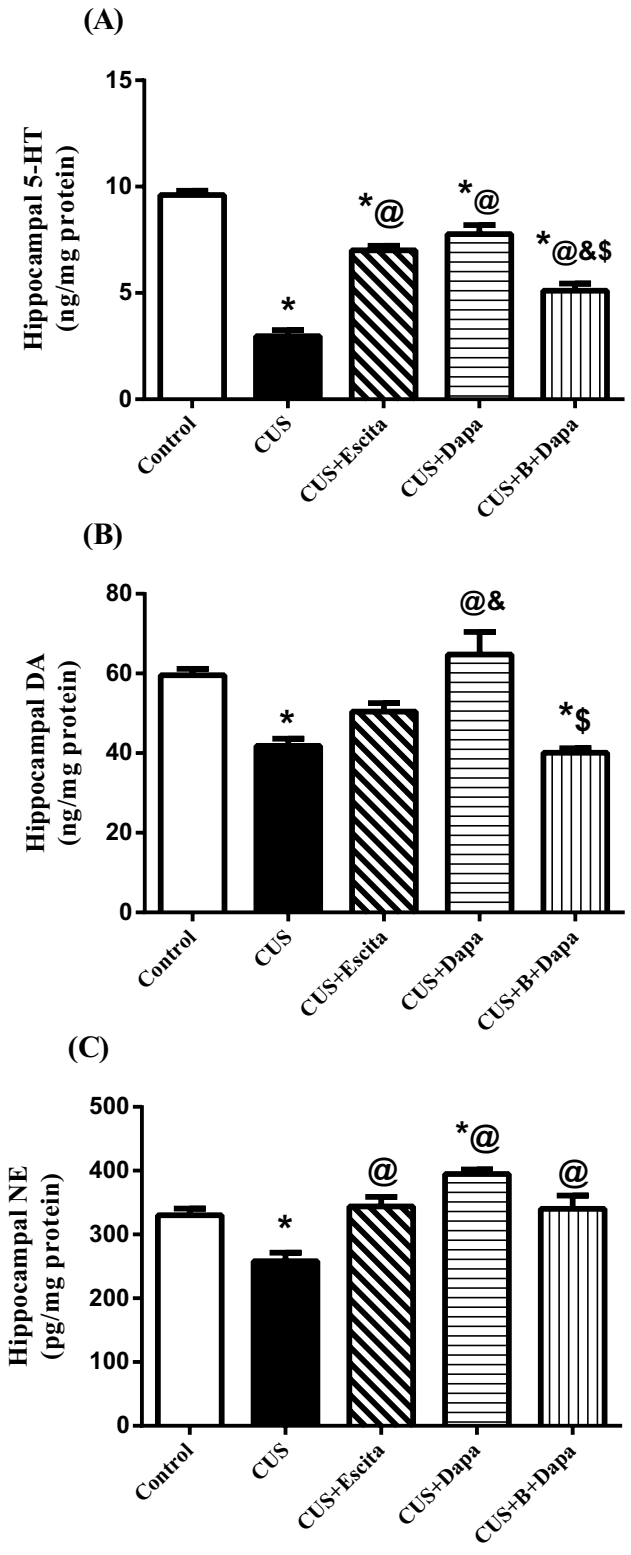

Fig. 3 Effect of the 5-week CUS protocol and co-treatments on hippocampal contents of **(a)** 5-HT, **(b)** DA, and **(c)** NE. Data is expressed as the mean of 7−8 experiments ± SEM, using one-way ANOVA with Tukey−Kramer multiple comparison post-test; as compared to normal (*), CUS (@), Escita (&), and Dapa ($)-treated groups ($p < 0.05$). 5-HT serotonin, B BQ-788, CUS chronic unpredictable stress, DA dopamine, Dapa dapagliflozin, Escita escitalopram, NE norepinephrine

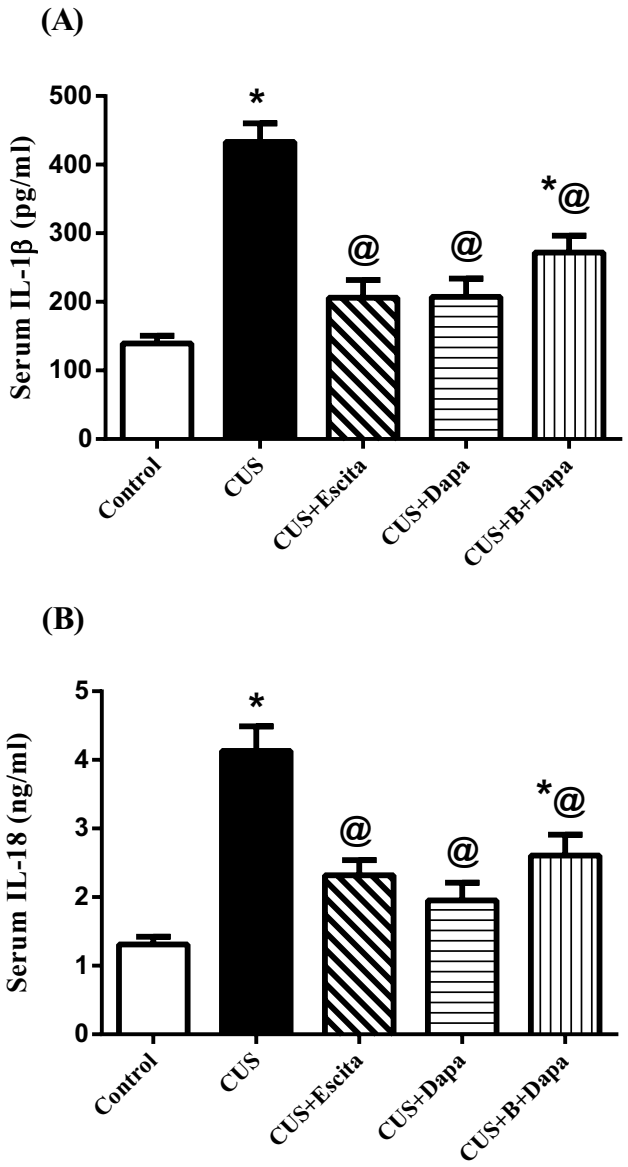

Fig. 4 Effect of the 5-week CUS protocol and co-treatments on serum levels of **(a)** IL-1β and **(b)** IL-18. Data is expressed as the mean of 7−8 experiments ± SEM, using one-way ANOVA with Tukey−Kramer multiple comparison post-test; as compared to normal (*), CUS (@), Escita (&), and Dapa ($)-treated groups ($p < 0.05$). B BQ-788, CUS chronic unpredictable stress, Dapa dapagliflozin, Escita escitalopram, IL interleukin

Although BQ-788 mitigated the overall effect of Dapa, none of its outcomes was significantly different, except for NF-κB (3-fold increase) and NLRP3 (approximately 2-fold increase), when compared to Dapa treatment.

Hippocampal ET System

Disturbances in the hippocampal ET system in the CUS group involved its three major components, viz., ET-1, ET_AR, and ET_BR (Fig. 6), wherein, compared to negative controls, ET-1

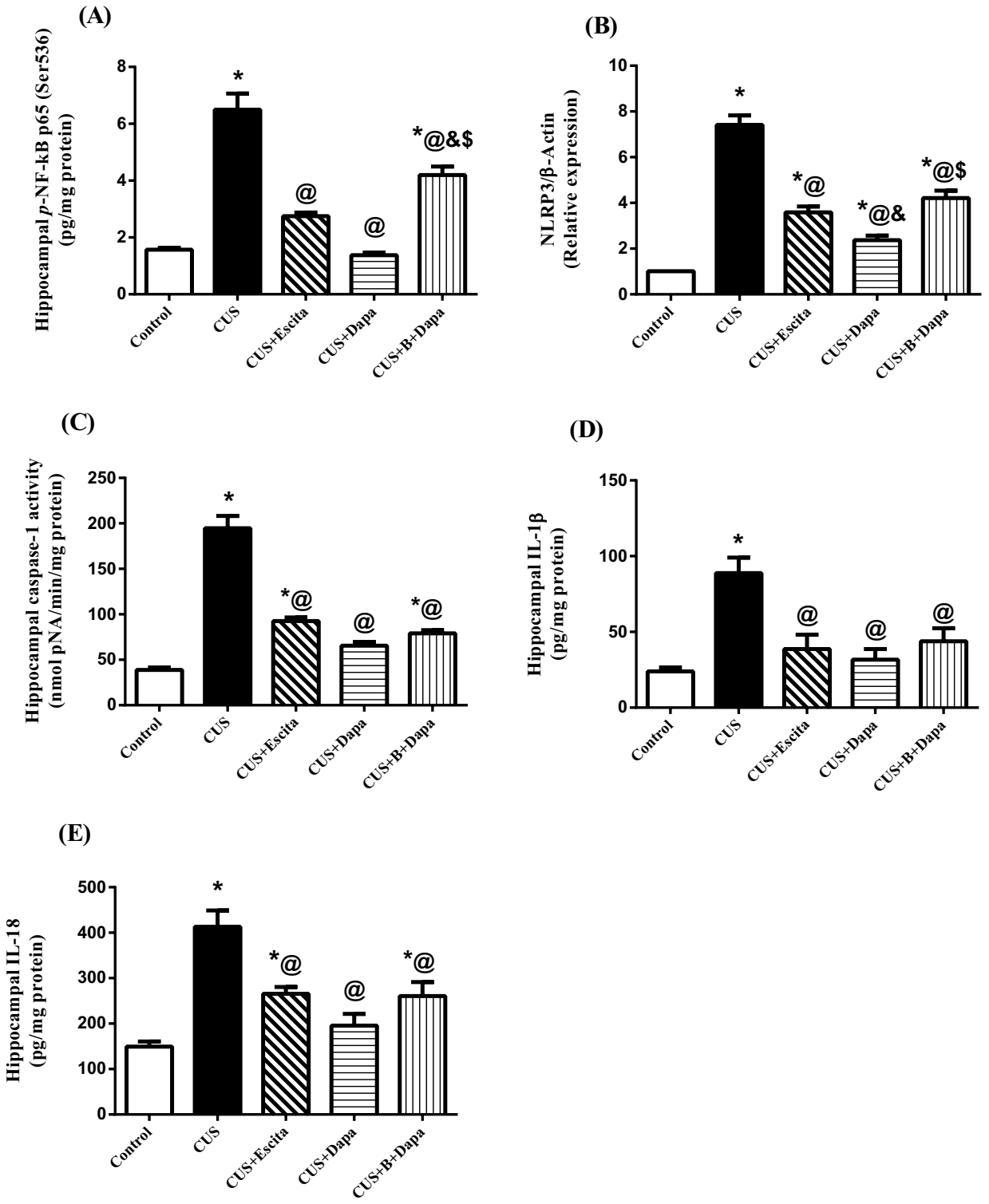

Fig. 5 Effect of the 5-week CUS protocol and co-treatments on hippocampal **(a)** *p*-NF-κB p65 (Ser536) content, **(b)** mRNA expression of NLRP3, **(c)** caspase-1 activity, **(d)** IL-1β, and **(e)** IL-18 contents. Data is expressed as the mean of 6 − 8 experiments ± SEM, using one-way ANOVA with Tukey−Kramer multiple comparison post-test; as compared to normal (*), CUS (@), Escita (&), and Dapa ($)-treated groups ($p < 0.05$). B BQ-788, CUS chronic unpredictable stress, Dapa dapagliflozin, Escita escitalopram, IL interleukin, *p*-NF-κB p65 (Ser536) phosphorylated nuclear factor-kappa B p65 at Ser 536, NLRP3 nucleotide-binding oligomerization domain, leucine-rich repeat and pyrin domain-containing protein 3

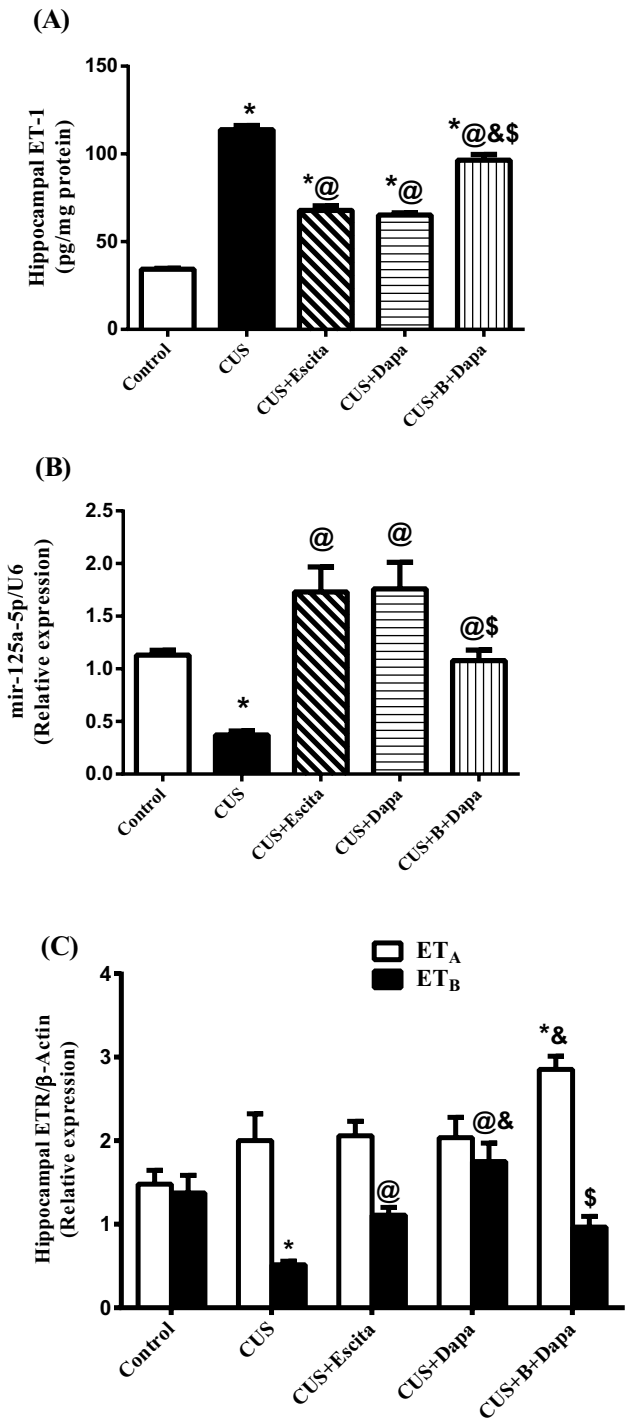

Fig. 6 Effect of the 5-week CUS protocol and co-treatments on hippocampal **(a)** ET-1 contents, **(b)** miR-125a-5p, and **(c)** ETR gene expressions. Data is expressed as the mean of 6 − 8 experiments ± SEM, using one-way ANOVA with Tukey−Kramer multiple comparison post-test; as compared to normal (*), CUS (@), Escita (&), and Dapa ($)-treated groups ($p < 0.05$). B BQ-788, CUS chronic unpredictable stress, Dapa dapagliflozin, Escita escitalopram, ET-1 endothelin-1, ETRs endothelin receptors

showed a prominent 3.3-fold elevation that corresponded to a 67% drop in miR-125a-5p, along with an ≈35% increase in the mRNA expression of ET_AR that was not statistically significant. In contrast, CUS was associated with a significant decline in the expression of ET_BR (37.5% of control value).

Co-treatment with Dapa significantly inhibited CUS-induced ET-1 elevation by 42.68% with a parallel increase in the expression of miR-125a-5p. Compared to CUS, Dapa did not considerably affect ET_AR expression, but it enhanced the expression of ET_BR by 239.08%. Congruent with these results, Escita exerted a significant yet weaker effect on hippocampal ET system components; i.e., it suppressed ET-1 by 40.44% and enhanced ET_BR expression by 114.68%, with no substantial effect on ET_AR.

BQ-788 almost completely abrogated the effect of Dapa as results were comparable to that of the CUS group.

BBB Integrity

Compared to normal controls, a significant increase in both cortical and hippocampal contents of TNF-α was revealed in the CUS group, with hippocampal contents being higher than those seen in the cortex (Fig. 7a). Further, cortical and hippocampal TNF-α increased by 38% and 66.23%, respectively, due to CUS, when compared to normal rats. Additionally, a prominent 3-fold escalation in the expression of cortical miR-501-3p was observed (Fig. 7b). In line with these results, the CUS protocol had a detrimental effect on cortical ZO-1 immunoreactivity, with a scarce presence of ZO-1-positive cells (Fig. 7c).

Treatment with Dapa was associated with remarkable modifications in these markers, as it led to a decrease in cortical and hippocampal TNF-α by 10% and 35.15%, respectively, and suppressed miR-501-3p expression by 91%. These outcomes were positively reflected in ZO-1 immunoreactivity, as Dapa treatment almost normalized the TJ protein expression with 10.4% area staining. These outcomes were analogous to those seen with Escita, except for ZO-1 expression, which was not at par with Dapa—percentage area stained was significantly lower at 8.7%.

Even though BQ-788 showed a positive outcome only on cortical TNF-α, displaying a further decrease compared to Dapa treatment, ZO-1 expression was, unexpectedly, severely affected and matched that of CUS.

Alterations in Hippocampal Neuroplasticity/ Synaptic Plasticity

CUS was detrimental to both neuronal and synaptic plasticity (Fig. 8) as it was associated with ≈23% and 59% decline in hippocampal BDNF and synapsin-1 contents, respectively. Dapa significantly elevated both BDNF (39.21%) and synapsin-1 (by 2.3-folds) contents compared to CUS,

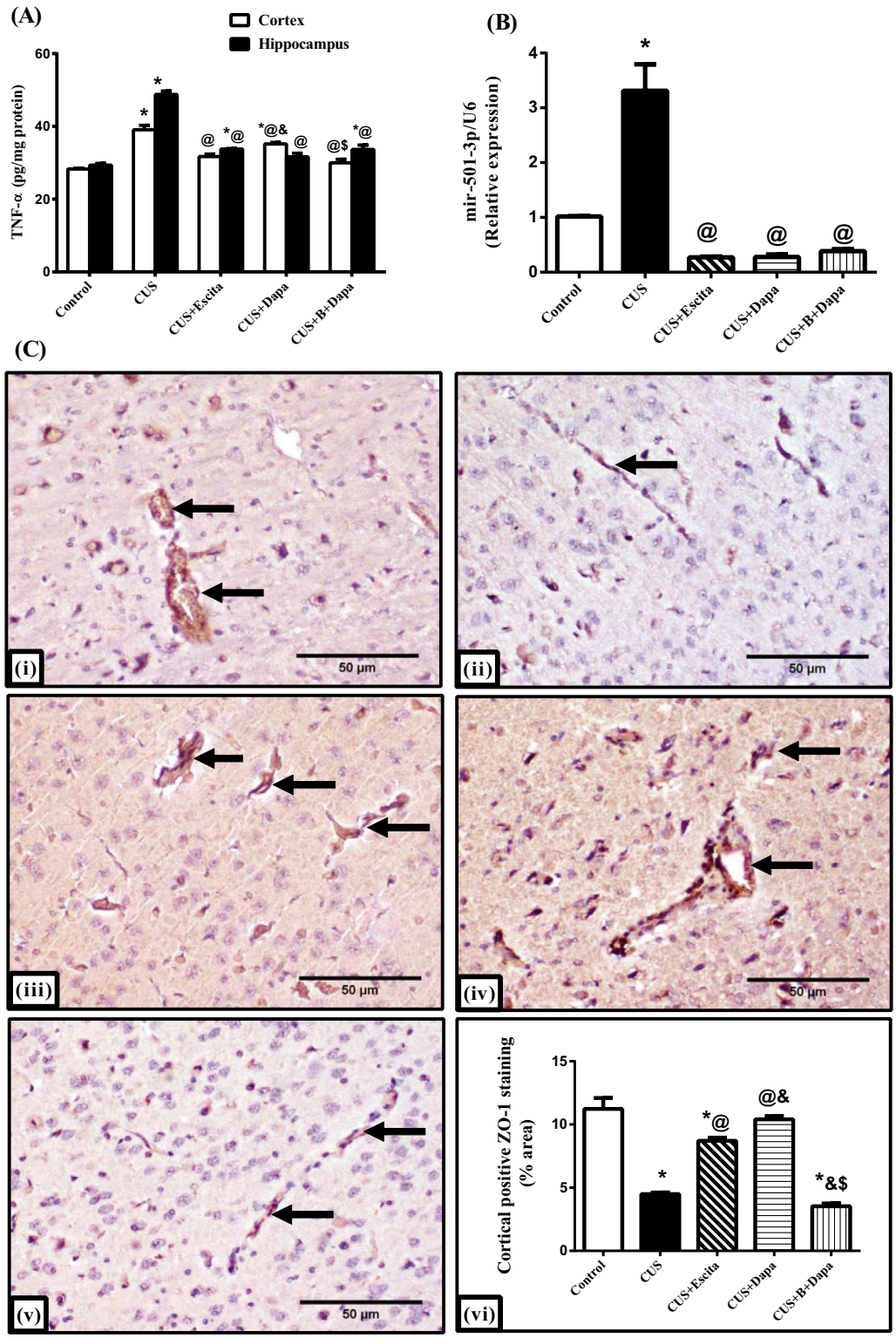

Fig. 7 Effect of CUS and co-treatments on **(a)** cortical/hippocampal TNF-α contents, **(b)** cortical miR-501-3p gene expression, and **(c)** cortical ZO-1 expression, where the representative photomicrographs ($n = 3$) of ZO-1 immuno-staining show microsections of **(i)** negative control, **(ii)** CUS, **(iii)** CUS + Escita, **(iv)** CUS + Dapa, and **(v)** CUS + B + Dapa (400×, scale bar 50 µm), with **(vi)** showing the percentage area staining. Data is expressed as the mean of 6 − 8 experiments ± SEM, using one-way ANOVA with Tukey−Kramer multiple comparison post-test; as compared to normal (*), CUS (@), Escita (&), and Dapa ($)-treated groups ($p < 0.05$). B BQ-788, CUS chronic unpredictable stress, Dapa dapagliflozin, Escita escitalopram, ZO-1 zonula occludens-1, TNF-α tumor necrosis factor-α

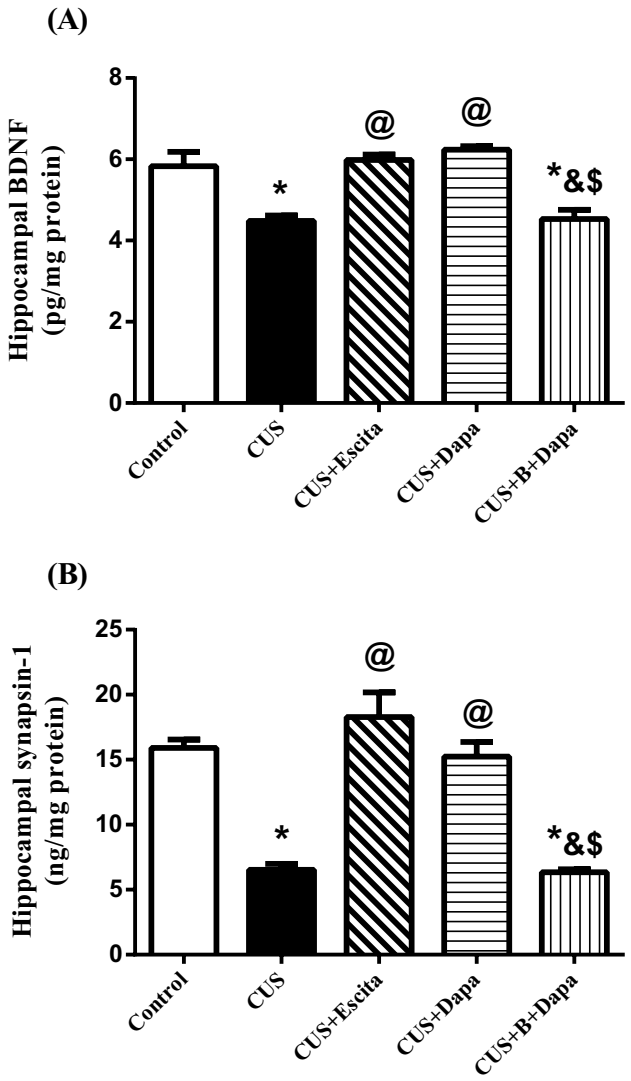

Fig. 8 Effect of CUS and co-treatments on hippocampal **(a)** BDNF and **(b)** synapsin-1 contents. Data is expressed as the mean of 7−8 experiments ± SEM, using one-way ANOVA with Tukey−Kramer multiple comparison post-test; as compared to normal (*), CUS (@), Escita (&), and Dapa ($)-treated groups ($p < 0.05$). B BQ-788, BDNF brain-derived neurotrophic factor, CUS chronic unpredictable stress, Dapa dapagliflozin, Escita escitalopram

and these results were almost identical to those obtained with Escita.

Finally, BQ-788 co-treatment led to a rigorous decline in both BDNF and synapsin-1 compared to Dapa, which was similar to that seen with CUS.

Cortical and Hippocampal Histopathological Findings

Compared to normal architecture seen in the control animals (Figs. 9a and 10a), those exposed to CUS showed altered histopathology, both in the cerebral cortex (Fig. 9b–d) and in the hippocampus (Fig. 10b). Cortical photomicrographs revealed severe neuropathic alterations that included perivascular and intracellular edema, necrosis of pyramidal neurons, vacuolation of the neuropil, pyknosis of granular cells, proliferation of glial cells, and neuronophagia (Fig. 9b–d). The severity of these neuropathic findings was nearly identical in the Dapa + BQ-788 group (Fig. 9g), though necrosis of the pyramidal neurons was the worst outcome. In contrast, marked regression of these neuropathic changes was observed in the cerebral cortex of Dapa-treated rats (Fig. 9f), as only slight vacuolation of the neuropil and sporadic necrosis of pyramidal neurons were observed. Meanwhile, the morphological picture of Escita-treated animals (Fig. 9e) was comparable to that seen with Dapa.

Light microscopy findings were identical in the hippocampus and the cortex. Both Dapa (Fig. 10d) and Escita (Fig. 10c) scored equally with respect to injury, but dark eosinophilic cytoplasm was only seen in Dapa + BQ-788 panels (Fig. 10e).

Discussion

In the present study, the antidepressant potential of Dapa, a SGLT2 inhibitor, was evaluated and our results not only highlight previously unexamined pathways in the pathogenesis of depression but also imply that this antidiabetic drug has concomitant positive outcomes on mental health, taking into consideration the high concurrence of depression in diabetic patients [6]. The well-established CUS model was utilized to induce depression-like symptoms in experimental animals. As this model has been frequently used, it is reliable, valid, relatively easy to apply, and indeed produces a wide array of neurobiological sequelae that reflect human depression [49, 50]. Here, Escita was used as a reference antidepressant agent, owing to largely consistent data on its efficacy and dosage in CUS models [37, 45].

The CUS protocol used here signified its detrimental effects on survival and weight gain, as previously observed [34]. It also revealed the anhedonic and despair features of depression on rats [8, 45, 51, 52]. However, in the OFT, no obvious differences were noted among the treated groups, although most of them showed higher ambulation and rearing frequencies as compared to controls. While these results are similar to those reported previously [34, 53], others have described opposite outcomes [34, 51, 54], which may be attributed to differences in CUS protocols and duration, and/or animal strain and age. Neurochemical alterations in the three estimated monoamines, i.e., 5-HT, DA, and NE in CUS-exposed rats, not only support the behavioral changes but also confirm progression of a depressive phenotype [34, 55, 56].

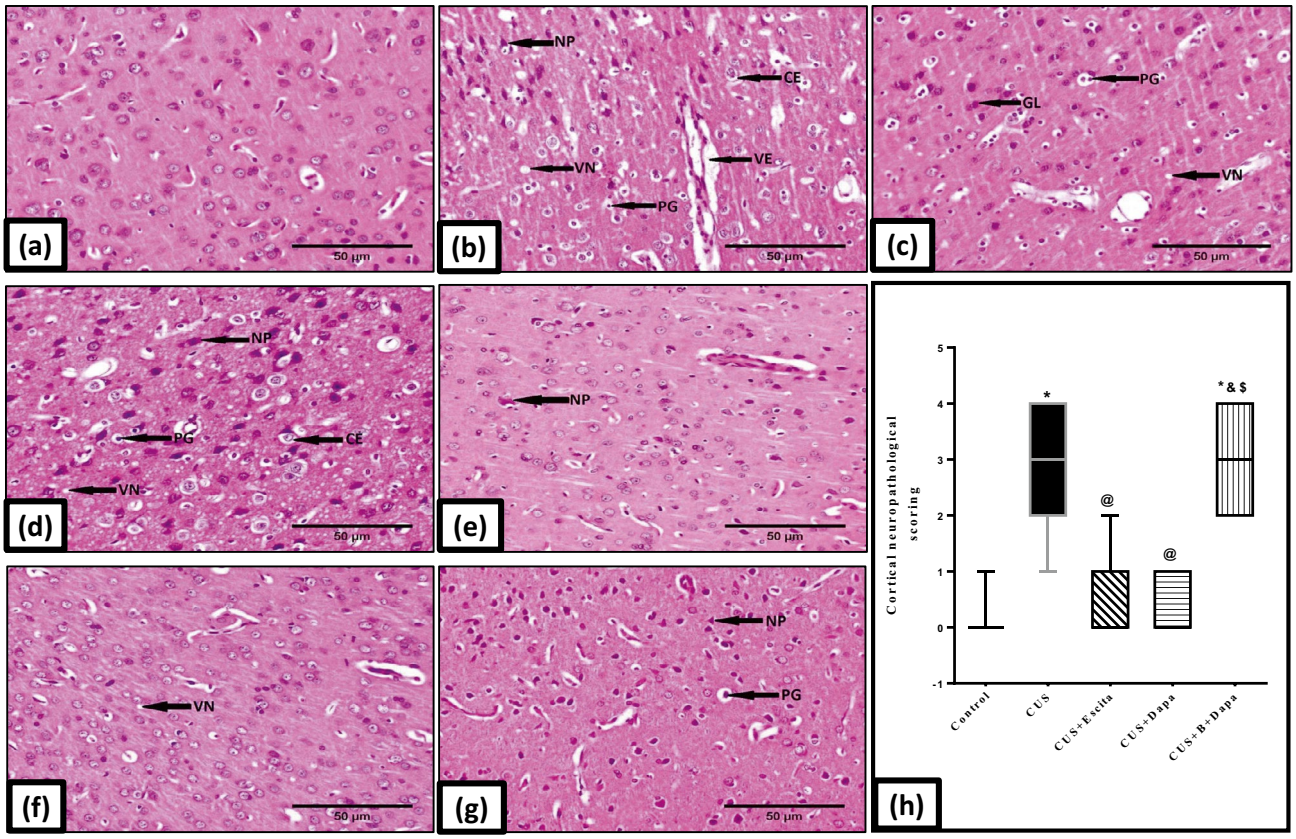

Fig. 9 Representative photomicrographs of H&E-stained microsections from the cerebral cortex ($n=3$). Pathological changes are indicated by black arrows in the panel. Slides from **(a)** negative control rats reveal normal architecture, while those obtained from **(b**, **c**, **d)** CUS group display necrosis of pyramidal neurons (NP), pyknosis of granular cells (PG), perivascular and intracellular edema (VE and CE, respectively), proliferation of glial cells (GL), and vacuolation of neuropil (VN). Marked necrosis of pyramidal neurons (NP) is the major feature in **(g)** BQ-788 + Dapa-treated rats, while both **(f)** Dapa and **(e)** Escita show only mild changes with neuronophagia (NH) being only seen in Escita (400×, scale bar 50 µm). The pathological scores are represented in panel **(h)**, where data is presented as box and whiskers by median (min−max) and 25^{th}–75^{th} percentile values using Kruskal–Wallis test with Dunn's multiple comparison post-test; as compared to normal (*), CUS (@), Escita (&), and Dapa ($)-treated groups ($p < 0.05$). B BQ-788, CUS chronic unpredictable stress, Dapa dapagliflozin, Escita escitalopram

Given the neuroimmune hypothesis of depression, previous studies have reported that CUS has detrimental peripheral effects [57, 58]; this was supported herein by the state of systemic inflammation as represented by elevated IL-1β and IL-18 levels. These cytokines, when peripherally elevated, are frequently associated with MDD and other mood disorders [2, 8, 12]. This systemic inflammation was reflected in brain biochemistry as well, specifically, by activation of the NLRP3 inflammasome pathway and the presence of congruent histopathological findings. Previous studies have documented the association between CUS and NLRP3 activation, which resulted in neuro-inflammation, impaired neurogenesis, and BBB disruption [12, 59–61]. Although basal expression of NLRP3 under normal conditions is not sufficient to activate the inflammasome, it can be upregulated by various stimuli, including NF-κB, and this is called the priming step [62]. Various studies have indeed identified NF-κB as a mediator of depressive behavior induced by CUS [63]. After priming and activation, pro-caspase-1 is proteolytically cleaved into active caspase-1 which in turn converts pro-IL-1β/IL-18 into their mature forms and initiates a highly inflammatory form of cell death, namely, pyroptosis [10–12, 62]. In a vicious cycle, both pyroptosis and IL-1β induce the assembly of additional inflammatory mediators, such as TNF-α [62]. This comes in accordance with our results where the entire NF-κB/NLRP3/caspase-1/IL-1β/IL-18/TNF-α axis was activated in the CUS group.

The stress protocol and resultant NLRP3 inflammasome activation were reflected in the ET system as hippocampal ET-1 levels were significantly increased, while ET_AR expression was only slightly elevated and ET_BR was suppressed. Only a few studies have addressed the link between the ET system and depression. Specifically, in two clinical studies, severe depressive symptoms were associated with high plasma ET-1 levels in post-acute coronary syndrome patients [64, 65], although an earlier study found no connection between the

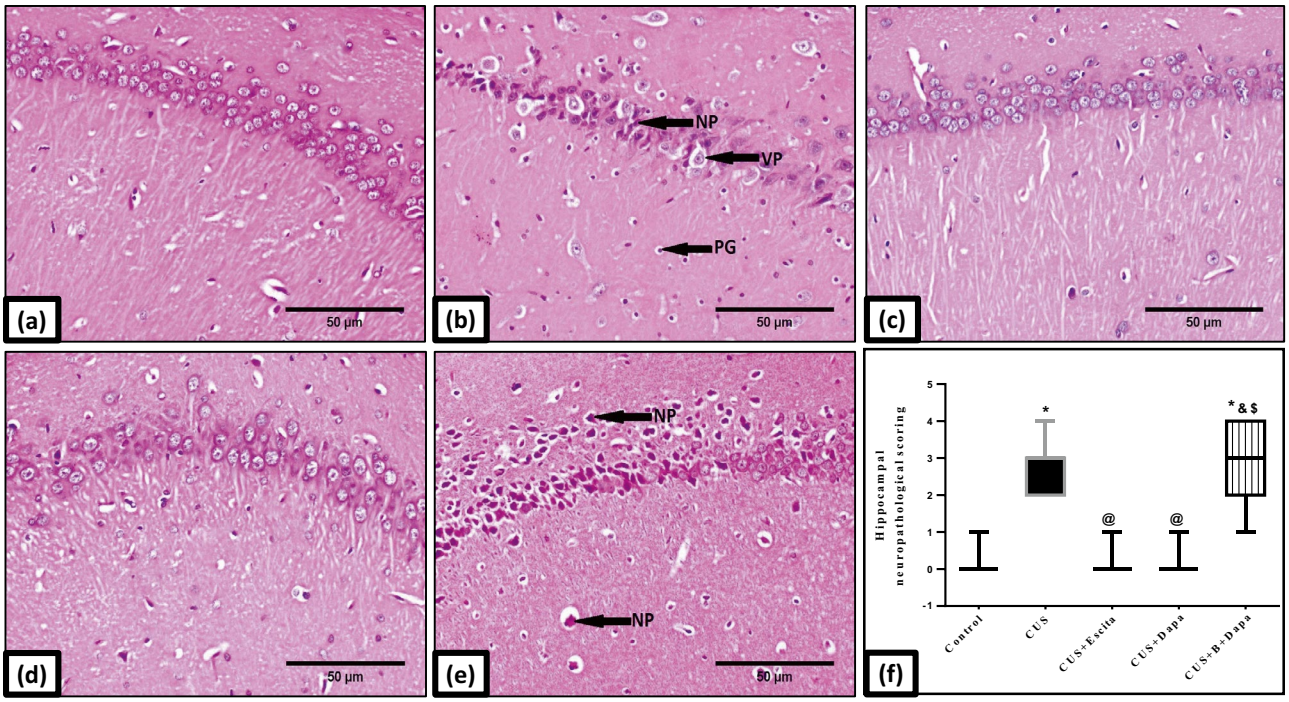

Fig. 10 Representative photomicrographs of H&E-stained microsections from hippocampal CA1 region ($n = 3$). Pathological changes are indicated by black arrows in the panel. Slides from **(a)** normal control rats reveal normal architecture, while those obtained from **(b)** CUS group display vacuolation and necrosis of pyramidal neurons (VP and NP, respectively) and pyknosis of granular cells (PG). The same findings were almost replicated in **(e)** BQ-788 + Dapa-treated rats, while both **(c)** Escita and **(d)** Dapa show no alterations (400×, scale bar 50 µm). The pathological scores are represented in panel **(f)**, where data is presented as box and whiskers by median (min−max) and 25^{th}–75^{th} percentile values using Kruskal–Wallis test with Dunn's multiple comparison post-test; as compared to normal (*), CUS (@), Escita (&), and Dapa ($)-treated groups ($p < 0.05$). B BQ-788, CUS chronic unpredictable stress, Dapa dapagliflozin, Escita escitalopram

two variables [66]. To the best of our knowledge, this is the first study to report a disturbance in the expression of hippocampal ETRs under the influence of stress. Loria et al. [67] have previously reported that early life stress in rats reduced peripheral expression of both ET_AR and ET_BR. Additionally, central ET_BR deficiency in rats was associated with higher constrictor response, increased apoptosis, and a decline in neural progenitor cells in the brain, emphasizing the importance of ET_BR in CNS development and maturity [68].

In the current study, higher ET-1 levels were correlated with activation of the NLRP3 pathway, which is contrary to the findings reported by Ward and Ergul [15]. Nevertheless, our findings are further strengthened by the fact that ET-1 release is strongly influenced by various inflammatory mediators, including IL-1β, TNF-α, and NF-κB [16], and that ET-1 itself was found to activate these molecules and increase their expression [69]. Hence, it appears that the relation between the NLRP3 inflammasome and the ET system is bi-directional [13, 14]. In the same context, ET-1 gene expression can be regulated by miRNAs, particularly miR-125a. This miRNA has been reported to negatively regulate not only ET-1 [21], but also the NLRP3 gene expression [70]. In congruence, miR-125a was found to be downregulated in the hippocampus of an animal model of chronic mild stress [71] and, conversely, its upregulation was associated with stronger BBB TJ complex formation [22]. These findings constitute adequate evidence for the use of miR-125a as a potential therapeutic target in MDD.

The previously mentioned trajectories were reflected on the main brain defense mechanisms, i.e., BBB integrity and neurogenesis/plasticity pathways. Our results revealed that CUS orchestrated multiple mechanisms that threatened the BBB. These include activation of the NLRP3 inflammasome pathway [9] and systemic inflammation, with consequent production of various cytokines that are known to negatively affect the BBB [62, 72]. Indeed, some studies have documented the deleterious effects of different psychological stressors on the BBB [72]. This was further aggravated herein by the disturbance caused by downregulation of miR-125a-5p and, conversely, upregulation of miR-501-3p, a miRNA through which TNF-α is thought to increase BBB leakage by suppressing ZO-1 [23, 24]. Finally, CUS repressed BDNF, a historic neurogenesis and plasticity mediator, and synapsin-1, a synaptic plasticity marker, which is in concordance with results from various studies [73, 74].

The antidepressant properties of Dapa were highly analogous to those of Escita, from behavioral observations to biochemical and histopathological findings. In this regard, Dapa abolished CUS-induced mortality and improved both weight gain and behavioral deteriorations. Moreover, Dapa reduced monoamine deficiency in the hippocampus—an outcome that can be linked to suppression of the NLRP3 inflammasome pathway and its associated ILs [12].

To be more specific, even though the anti-inflammatory properties of Dapa and other SGLT2 inhibitors are well-documented [28, 29], little is known about their ability to attenuate the NLRP3 inflammasome that potentially represents a promising therapeutic target for SGLT2 inhibitors [75, 76]. Interestingly, standard antidepressants have recently been recognized for their ability to modulate this pathway and, thereby attenuate the inflammatory response and promote stress resilience [77]. In this context, Dapa demonstrated its strong anti-inflammatory potential both peripherally by suppressing ILs overproduction and centrally by hindering the NLRP3 inflammasome activation axis. More importantly, histopathological findings seen with Dapa supported these biochemical outcomes.

Dapa was found to restore the disturbed ET system. Though Dapa has been previously reported to improve endothelial dysfunction [78], no evidence regarding its suppressive effect on ET-1 has been documented. Nonetheless, this effect can be explained by the established anti-inflammatory potential of Dapa and its ability to suppress various cytokines known to stimulate ET-1 production [78]; importantly, these cytokines represent end products of the NLRP3 inflammasome cascade. The ability of Dapa to normalize both miR-125a-5p and ET_BR expression is an additional merit that reflected in both neurotrophins production and BBB maintenance. Additionally, Dapa conceivably enhanced ZO-1 expression through modulation of the NLRP3/TNF-α/miR-501-3p/ZO-1 axis.

Based on all these advantages, it was not surprising for Dapa to outstandingly boost levels of both BDNF and synapsin-1. In fact, Lin et al. [79] have reported that empagliflozin, a SGLT2 inhibitor, enhanced cerebral BDNF in diabetic obese mice; however, the mechanism mediating this effect was not clear. Given the established role of ET_BR signaling in controlling neurogenesis and synaptogenesis [16, 39, 80], our observations confirm that BQ-788 + Dapa remarkably reduced both BDNF and synapsin-1 levels and worsened not only the histopathology but also behavioral outcomes. Even though a strong body of evidence supports the positive relation between ET_BR blockade and the BBB integrity, our findings are not in the favor of this hypothesis, which can be explained by BDNF deficiency secondary to BQ-788 co-treatment [81, 82]. BDNF preserves endothelial and intestinal mucosal barrier functions, and its deficiency is correlated with lower ZO-1 expression [81, 82]. As BQ-788 treatment reversed most of the positive outcomes associated with Dapa herein, ET_BR signaling could represent a core feature by which Dapa enhanced neuroplasticity and promoted stress resilience in rats.

Conclusion

The prevalent resistance to traditional antidepressants necessitates the development of novel therapies that go beyond the idea of deficient monoamines and focus on innovative mechanisms that promote stress resilience. Dapa, a SGLT2 inhibitor, has drawn the attention towards its benefits on CNS. Our results imply that the NLRP3 inflammasome may be a promising therapeutic target for depression and that Dapa can significantly suppress its activation to halt both neuro-inflammation and BBB disturbance, mediated through the NLRP3/IL/TNF-α/miR-501-3p/ZO-1 axis. Additionally, we demonstrate herein, for the first time, a significant role of ET_BR signaling in mediating neuroplasticity upon Dapa treatment via the miR-125a-5p/ET-1/ET_BR/BDNF/synapsin-1 signal transduction pathway.

Supplementary Information The online version contains supplementary material available at https://doi.org/10.1007/s13311-021-01140-4.

Author Contribution R.N.M. perceived the study. R.N.M., L.A.A., R.M.A., and A.S.A. jointly constructed the experiments. R.N.M. carried out the experiments. R.N.M. and L.A.A. executed the statistical analysis. R.N.M. and L.A.A. deduced the data and wrote the manuscript. R.M.A. and A.S.A. provided technical support and revised the manuscript. K.A.A. performed all histopathological and immunohistochemical examinations, imaging, and analysis. All authors accepted the final version of the manuscript and approved to be responsible for all aspects of the work.

Required Author Forms Disclosure forms provided by the authors are available with the online version of this article.

Declarations

Conflict of Interest The authors declare no competing interests.

References

1. Disease GBD, Injury I, Prevalence C. Global, regional, and national incidence, prevalence, and years lived with disability for 354 diseases and injuries for 195 countries and territories, 1990-2017: a systematic analysis for the Global Burden of Disease Study 2017. Lancet. 2018;392:1789-1858.
2. Pitsillou E, Bresnehan SM, Kagarakis EA, Wijoyo SJ, Liang J, Hung A, *et al.* The cellular and molecular basis of major depressive disorder: towards a unified model for understanding clinical depression. Mol Biol Rep. 2020;47:753-770.

3. Herzog DP, Beckmann H, Lieb K, Ryu S, Müller MB. Understanding and Predicting Antidepressant Response: Using Animal Models to Move Toward Precision Psychiatry. Front Psychiatry. 2018;9:512. https://doi.org/10.3389/fpsyt.2018.00512.
4. Kennedy SH. Core symptoms of major depressive disorder: relevance to diagnosis and treatment. Dialogues Clin Neurosci. 2008;10:271-277.
5. Alessio Filippo P, Rosalia C, Maria S, Enrico G, Rosalba S, Daniela I, *et al.* The Role of Annexin A1 and Formyl Peptide Receptor 2/3 Signaling in Chronic Corticosterone-Induced Depression-Like behaviors and Impairment in Hippocampal-Dependent Memory. CNS Neurol Disord - Drug Targets. 2020;19:27-43.
6. Bădescu SV, Tătaru C, Kobylinska L, Georgescu EL, Zahiu DM, Zăgrean AM, *et al.* The association between Diabetes mellitus and Depression. J Med Life. 2016;9:120-125.
7. Van Dyken P, Lacoste B. Impact of Metabolic Syndrome on Neuroinflammation and the Blood-Brain Barrier. Front Neurosci. 2018;12:930. https://doi.org/10.3389/fnins.2018.00930. eCollection 2018.
8. Menard C, Hodes GE, Russo SJ. Pathogenesis of depression: Insights from human and rodent studies. Neuroscience. 2016;321:138-162.
9. Wang H, Chen H, Jin J, Liu Q, Zhong D, Li G. Inhibition of the NLRP3 inflammasome reduces brain edema and regulates the distribution of aquaporin-4 after cerebral ischaemia-reperfusion. Life Sci. 2020;251:117638. https://doi.org/10.1016/j.lfs.2020.117638.
10. Cordaro M, Fusco R, D'Amico R, Siracusa R, Peritore AF, Gugliandolo E, *et al.* Cashew (Anacardium occidentale L.) Nuts Modulate the Nrf2 and NLRP3 Pathways in Pancreas and Lung after Induction of Acute Pancreatitis by Cerulein. Antioxidants. 2020;9:992. https://doi.org/10.3390/antiox9100992.
11. D'Amico R, Fusco R, Cordaro M, Siracusa R, Peritore AF, Gugliandolo E, *et al.* Modulation of NLRP3 Inflammasome through Formyl Peptide Receptor 1 (Fpr-1) Pathway as a New Therapeutic Target in Bronchiolitis Obliterans Syndrome. Int J of Mol Sci. 2020;21:2144. https://doi.org/10.3390/ijms21062144.
12. Kaufmann FN, Costa AP, Ghisleni G, Diaz AP, Rodrigues ALS, Peluffo H, *et al.* NLRP3 inflammasome-driven pathways in depression: Clinical and preclinical findings. Brain Behav Immun. 2017;64:367-383.
13. Fais RS, Gomes RF, Wanderley CW, Tostes Rd, Carneiro FS. Nlrp3 Activation by Endothelin-1 Mediates Neutrophil Recruitment in Cavernosal Tissue of DOCA/salt Mice. Hypertension. 2019;74(suppl 3): P124-Abstract.
14. Gora IM, Ciechanowska A. NLRP3 Inflammasome at the Interface of Inflammation, Endothelial Dysfunction, and Type 2 Diabetes. Cells. 2021;10: 314. https://doi.org/10.3390/cells10020314.
15. Ward R, Ergul A. Relationship of endothelin-1 and NLRP3 inflammasome activation in HT22 hippocampal cells in diabetes. Life Sci. 2016;159:97-103.
16. Koyama Y. Endothelin systems in the brain: involvement in pathophysiological responses of damaged nerve tissues. Biomol Concepts. 2013;4:335-347.
17. Gulati A. Endothelin Receptors, Mitochondria and Neurogenesis in Cerebral Ischemia. Curr Neuropharmacol. 2016;14:619-626.
18. Michinaga S, Inoue A, Yamamoto H, Ryu R, Inoue A, Mizuguchi H, *et al.* Endothelin receptor antagonists alleviate blood-brain barrier disruption and cerebral edema in a mouse model of traumatic brain injury: A comparison between bosentan and ambrisentan. Neuropharmacology. 2020;175:108182. https://doi.org/10.1016/j.neuropharm.2020.108182.
19. Chuquet J, Benchenane K, Toutain J, MacKenzie ET, Roussel S, Touzani O. Selective blockade of endothelin-B receptors exacerbates ischemic brain damage in the rat. Stroke. 2002;33:3019-3025.
20. Chen M, Yan H-h, Shu S, Pei L, Zang L-k, Fu Y, *et al.* Amygdalar Endothelin-1 Regulates Pyramidal Neuron Excitability and Affects Anxiety. Sci Rep. 2017;7:2316. https://doi.org/10.1038/s41598-017-02583-6.
21. Jacobs ME, Wingo CS, Cain BD. An emerging role for microRNA in the regulation of endothelin-1. Front Physiol. 2013;4:22. https://doi.org/10.3389/fphys.2013.00022. eCollection 2013.
22. Petrescu GED, Sabo AA, Torsin LI, Calin GA, Dragomir MP. MicroRNA based theranostics for brain cancer: basic principles. J Exp Clin Cancer Res. 2019;38:231. https://doi.org/10.1186/s13046-019-1180-5.
23. Toyama K, Spin JM, Deng AC, Huang TT, Wei K, Wagenhauser MU, *et al.* MicroRNA-Mediated Therapy Modulating Blood-Brain Barrier Disruption Improves Vascular Cognitive Impairment. Arterioscler Thromb Vasc Biol. 2018;38:1392-1406.
24. Yuan M, Bi X. Therapeutic and Diagnostic Potential of microRNAs in Vascular Cognitive Impairment. J Mol Neurosci. 2020;70:1619-1628.
25. Arosio B, Guerini FR, Voshaar RCO, Aprahamian I. Blood Brain-Derived Neurotrophic Factor (BDNF) and Major Depression: Do We Have a Translational Perspective? Front Behav Neurosci. 2021;15:626906. https://doi.org/10.3389/fnbeh.2021.626906.
26. Abdul-Ghani MA, DeFronzo RA. Inhibition of renal glucose reabsorption: a novel strategy for achieving glucose control in type 2 diabetes mellitus. Endocr Pract. 2008;14:782-790.
27. Idris I, Donnelly R. Sodium–glucose co-transporter-2 inhibitors: an emerging new class of oral antidiabetic drug. Diabetes, Obes and Metab. 2009;11:79-88.
28. Vasquez-Rios G, Nadkarni GN. SGLT2 Inhibitors: Emerging Roles in the Protection Against Cardiovascular and Kidney Disease Among Diabetic Patients. Int J Nephrol Renovasc Dis. 2020;13:281-296.
29. Sa-Nguanmoo P, Tanajak P, Kerdphoo S, Jaiwongkam T, Pratchayasakul W, Chattipakorn N, *et al.* SGLT2-inhibitor and DPP-4 inhibitor improve brain function via attenuating mitochondrial dysfunction, insulin resistance, inflammation, and apoptosis in HFD-induced obese rats. Toxicol Appl Pharmacol. 2017;333:43-50.
30. Wiciński M, Wódkiewicz E. Perspective of SGLT2 Inhibition in Treatment of Conditions Connected to Neuronal Loss: Focus on Alzheimer's Disease and Ischemia-Related Brain Injury. Pharmaceuticals (Basel). 2020;13:379. https://doi.org/10.3390/ph13110379.
31. Esterline R, Oscarsson J, Burns J. A role for sodium glucose cotransporter 2 inhibitors (SGLT2is) in the treatment of Alzheimer's disease? Int Rev Neurobiol. 2020;155:113-140.
32. El-Sahar AE, Rastanawi AA, El-Yamany MF, Saad MA. Dapagliflozin improves behavioral dysfunction of Huntington's disease in rats via inhibiting apoptosis-related glycolysis. Life Sci. 2020;257:118076. https://doi.org/10.1016/j.lfs.2020.118076.
33. Shaikh S, Rizvi SM, Shakil S, Riyaz S, Biswas D, Jahan R. Forxiga (dapagliflozin): Plausible role in the treatment of diabetes-associated neurological disorders. Biotechnol Appl Biochem. 2016;63:145-150.
34. Sequeira-Cordero A, Salas-Bastos A, Fornaguera J, Brenes JC. Behavioural characterisation of chronic unpredictable stress based on ethologically relevant paradigms in rats. Sci Rep. 2019;9:17403. https://doi.org/10.1038/s41598-019-53624-1.
35. Schneider M. Adolescence as a vulnerable period to alter rodent behavior. Cell Tissue Res. 2013;354:99-106.
36. Ibrahim WW, Safar MM, Khattab MM, Agha AM. 17β-Estradiol augments antidepressant efficacy of escitalopram in ovariectomized rats: Neuroprotective and serotonin reuptake transporter modulatory effects. Psychoneuroendocrinology. 2016;74:240-250.
37. Bondi CO, Rodriguez G, Gould GG, Frazer A, Morilak DA. Chronic unpredictable stress induces a cognitive deficit and anxiety-like behavior in rats that is prevented by chronic antidepressant drug treatment. Neuropsychopharmacology. 2008;33:320-331.
38. Briyal S, Nguyen C, Leonard M, Gulati A. Stimulation of endothelin B receptors by IRL-1620 decreases the progression of Alzheimer's disease. Neuroscience. 2015;301:1-11.
39. Leonard MG, Gulati A. Endothelin B receptor agonist, IRL-1620, enhances angiogenesis and neurogenesis following cerebral ischemia in rats. Brain Res. 2013;1528:28-41.

40. Belovicova K, Bogi E, Csatlosova K, Dubovicky M. Animal tests for anxiety-like and depression-like behavior in rats. Interdiscip Toxicol. 2017;10:40-43.
41. Zhang Y, Wang Y, Wang L, Bai M, Zhang X, Zhu X. Dopamine Receptor D2 and Associated microRNAs Are Involved in Stress Susceptibility and Resistance to Escitalopram Treatment. Int J Neuropsychopharmacol. 2015;18:pyv025. https://doi.org/10.1093/ijnp/pyv025.
42. Scheggi S, De Montis MG, Gambarana C. Making Sense of Rodent Models of Anhedonia. Int J Neuropsychopharmacol. 2018;21:1049-1065.
43. Casarotto PC, Andreatini R. Repeated paroxetine treatment reverses anhedonia induced in rats by chronic mild stress or dexamethasone. Eur Neuropsychopharmacol. 2007;17:735-742.
44. Liu M-Y, Yin C-Y, Zhu L-J, Zhu X-H, Xu C, Luo C-X, *et al.* Sucrose preference test for measurement of stress-induced anhedonia in mice. Nat Protoc. 2018;13:1686-1698.
45. Han Y, Deng X, Zhang Y, Wang X, Zhu X, Mei S, *et al.* Antidepressant-like effect of flaxseed in rats exposed to chronic unpredictable stress. Brain Behav. 2020;10:e01626. https://doi.org/10.1002/brb3.1626.
46. Slattery DA, Cryan JF. Using the rat forced swim test to assess antidepressant-like activity in rodents. Nat Protoc. 2012;7:1009-1014.
47. Thoresen M, Bågenholm R, Løberg EM, Apricena F, Kjellmer I. Posthypoxic cooling of neonatal rats provides protection against brain injury. Arch Dis Child Fetal Neonatal Ed. 1996;74:F3-F9.
48. El-Shiekh RA, Ashour RM, Abd El-Haleim EA, Ahmed KA, Abdel-Sattar E. Hibiscus sabdariffa L.: A potent natural neuroprotective agent for the prevention of streptozotocin-induced Alzheimer's disease in mice. Biomed Pharmacother. 2020;128:110303. https://doi.org/10.1016/j.biopha.2020.110303.
49. Hao Y, Ge H, Sun M, Gao Y. Selecting an Appropriate Animal Model of Depression. Int J Mol Sci. 2019;20:4827. https://doi.org/10.3390/ijms20194827.
50. Planchez B, Surget A, Belzung C. Animal models of major depression: drawbacks and challenges. J Neural Transm. 2019;126:1383-1408.
51. Wang D, An SC, Zhang X. Prevention of chronic stress-induced depression-like behavior by inducible nitric oxide inhibitor. Neurosci Lett. 2008;433:59-64.
52. Du X, Yin M, Yuan L, Zhang G, Fan Y, Li Z, *et al.* Reduction of depression-like behavior in rat model induced by ShRNA targeting norepinephrine transporter in locus coeruleus. Transl Psychiatry. 2020;10:130. https://doi.org/10.1038/s41398-020-0808-8.
53. Harris RBS, Zhou J, Youngblood BD, Smagin GN, Ryan DH. Failure to Change Exploration or Saccharin Preference In Rats Exposed to Chronic Mild Stress. Physiol Behav. 1997;63:91-100.
54. D'Aquila PS, Peana AT, Carboni V, Serra G. Exploratory behaviour and grooming after repeated restraint and chronic mild stress: effect of desipramine. Eur J Pharmacol. 2000;399:43-47.
55. Hill MN, Hellemans KGC, Verma P, Gorzalka BB, Weinberg J. Neurobiology of chronic mild stress: parallels to major depression. Neurosci Biobehav Rev. 2012;36:2085-2117.
56. Willner P. Chronic mild stress (CMS) revisited: consistency and behavioural-neurobiological concordance in the effects of CMS. Neuropsychobiology. 2005;52:90-110.
57. López-López AL, Jaime HB, Escobar Villanueva MdC, Padilla MB, Palacios GV, Aguilar FJA. Chronic unpredictable mild stress generates oxidative stress and systemic inflammation in rats. Physiol Behav. 2016;161:15–23.
58. Wei L, Li Y, Tang W, Sun Q, Chen L, Wang X, *et al.* Chronic Unpredictable Mild Stress in Rats Induces Colonic Inflammation. Front Physiol. 2019;10: 1228. https://doi.org/10.3389/fphys.2019.01228.
59. Yamanashi T, Iwata M, Kamiya N, Tsunetomi K, Kajitani N, Wada N, *et al.* Beta-hydroxybutyrate, an endogenic NLRP3 inflammasome inhibitor, attenuates stress-induced behavioral and inflammatory responses. Sci Rep. 2017;7:7677. https://doi.org/10.1038/s41598-017-08055-1.
60. Pasinetti G. Flavonoids Ameliorate Stress-Induced Depression by Preventing NLRP3 Inflammasome Priming. Curr Dev Nutr. 2020;4(suppl 2):1231. Abstract.
61. Yue N, Huang H, Zhu X, Han Q, Wang Y, Li B, *et al.* Activation of P2X7 receptor and NLRP3 inflammasome assembly in hippocampal glial cells mediates chronic stress-induced depressive-like behaviors. J Neuroinflammation. 2017;14:102. https://doi.org/10.1186/s12974-017-0865-y.
62. Song L, Pei L, Yao S, Wu Y, Shang Y. NLRP3 Inflammasome in Neurological Diseases, from Functions to Therapies. Front Cell Neurosci. 2017;11:63. https://doi.org/10.3389/fncel.2017.00063. eCollection 2017.
63. Koo JW, Russo SJ, Ferguson D, Nestler EJ, Duman RS. Nuclear factor-kappaB is a critical mediator of stress-impaired neurogenesis and depressive behavior. Proc Natl Acad Sci USA. 2010;107:2669-2674.
64. Burg MM, Martens EJ, Collins D, Soufer R. Depression predicts elevated endothelin-1 in patients with coronary artery disease. Psychosom Med. 2011;73:2-6.
65. Yammine L, Frazier L, Padhye NS, Burg MM, Meininger JC. Severe depressive symptoms are associated with elevated endothelin-1 in younger patients with acute coronary syndrome. J Psychosom Res. 2014;77:430-434.
66. Lederbogen F, Weber B, Colla M, Heuser I, Deuschle M. Endothelin-1 Plasma Concentrations in Depressed Patients and Healthy Controls. Neuropsychobiology. 1999;40:121-123.
67. Loria AS, D'Angelo G, Pollock DM, Pollock JS. Early life stress downregulates endothelin receptor expression and enhances acute stress-mediated blood pressure responses in adult rats. Am J Physiol Regul Integr Comp Physiol. 2010;299:R185-191.
68. Gulati A, Hornick MG, Briyal S, Lavhale MS. A novel neuroregenerative approach using ET(B) receptor agonist, IRL-1620, to treat CNS disorders. Physiol Res. 2018;67:S95-S113.
69. Kowalczyk A, Kleniewska P, Kolodziejczyk M, Skibska B, Goraca A. The role of endothelin-1 and endothelin receptor antagonists in inflammatory response and sepsis. Arch Immunol Ther Exp (Warsz). 2015;63:41-52.
70. Wang J, Wu Q, Yu J, Cao X, Xu Z. miR-125a-5p inhibits the expression of NLRP3 by targeting CCL4 in human vascular smooth muscle cells treated with ox-LDL. Exp Ther Med. 2019;18:1645-1652.
71. Dwivedi Y. Emerging role of microRNAs in major depressive disorder: diagnosis and therapeutic implications. Dialogues Clin Neurosci. 2014;16:43-61.
72. Welcome MO, Mastorakis NE. Stress-induced blood brain barrier disruption: Molecular mechanisms and signaling pathways. Pharmacol Res. 2020;157:104769. https://doi.org/10.1016/j.phrs.2020.104769.
73. Zhang X, Xue Y, Li J, Xu H, Yan W, Zhao Z, *et al.* The involvement of ADAR1 in antidepressant action by regulating BDNF via miR-432. Behav Brain Res. 2021;402:113087. https://doi.org/10.1016/j.bbr.2020.113087.
74. Dagyte G, Luiten PG, De Jager T, Gabriel C, Mocaër E, Den Boer JA, *et al.* Chronic stress and antidepressant agomelatine induce region-specific changes in synapsin I expression in the rat brain. J Neurosci Res. 2011;89:1646-1657.
75. Ye Y, Bajaj M, Yang HC, Perez-Polo JR, Birnbaum Y. SGLT-2 Inhibition with Dapagliflozin Reduces the Activation of the Nlrp3/ASC Inflammasome and Attenuates the Development of Diabetic Cardiomyopathy in Mice with Type 2 Diabetes. Further Augmentation of the Effects with Saxagliptin, a DPP4 Inhibitor. Cardiovasc Drugs Ther. 2017;31:119–132.
76. Sharma A, Tate M, Mathew G, Vince JE, Ritchie RH, de Haan JB. Oxidative Stress and NLRP3-Inflammasome Activity as Significant Drivers of Diabetic Cardiovascular Complications: Therapeutic

Implications. Front Physiol. 2018;9. https://doi.org/10.3389/fphys.2018.00114.
77. Szałach ŁP, Lisowska KA, Cubała WJ. The Influence of Antidepressants on the Immune System. Arch Immunol Ther Exp (Warsz). 2019;67:143-151.
78. Alshnbari AS, Millar SA, O'Sullivan SE, Idris I. Effect of Sodium-Glucose Cotransporter-2 Inhibitors on Endothelial Function: A Systematic Review of Preclinical Studies. Diabetes Ther. 2020;11:1947-1963.
79. Lin B, Koibuchi N, Hasegawa Y, Sueta D, Toyama K, Uekawa K, *et al.* Glycemic control with empagliflozin, a novel selective SGLT2 inhibitor, ameliorates cardiovascular injury and cognitive dysfunction in obese and type 2 diabetic mice. Cardiovasc Diabetol. 2014;13:148. https://doi.org/10.1186/s12933-014-0148-1.
80. Van Bulck M, Sierra-Magro A, Alarcon-Gil J, Perez-Castillo A, Morales-Garcia JA. Novel Approaches for the Treatment of Alzheimer's and Parkinson's Disease. Int J Mol Sci. 2019;20:719. https://doi.org/10.3390/ijms20030719.
81. Matsuda S, Fujita T, Kajiya M, Kashiwai K, Takeda K, Shiba H, *et al*. Brain-derived neurotrophic factor prevents the endothelial barrier dysfunction induced by interleukin-1β and tumor necrosis factor-α. J Periodontal Res. 2015;50:444-451.
82. Li C, Cai YY, Yan ZX. Brain-derived neurotrophic factor preserves intestinal mucosal barrier function and alters gut microbiota in mice. Kaohsiung J Med Sci. 2018;34:134-141.